

The crossover from classical to quantum transport in a weakly-interacting Fermi gas

Hadrien Kurkjian¹

¹*Laboratoire de Physique Théorique de la Matière Condensée,*

*Sorbonne Université, CNRS, 75005, Paris, France**

We present an exact solution of the quantum kinetic equation of a weakly interacting Fermi gas in the crossover from the degenerate Fermi-liquid regime to the classical Boltzmann gas. We construct families of orthogonal polynomials tailored to each angular momentum channel, enabling a fast and systematically improvable decomposition of the phase-space distribution. This approach yields accurate, non-variational predictions for the shear viscosity, thermal diffusivity, and spin diffusivity to leading order in the scattering length. We demonstrate that the commonly used relaxation-time approximation fails dramatically at low temperature—by up to 25%. Our method provides a numerically efficient framework for benchmarking transport in strongly correlated regimes and for simulating the kinetics of quantum gases beyond hydrodynamics.

INTRODUCTION

A weakly-interacting Fermi gas smoothly interpolates between a Fermi liquid at low temperatures, and a Boltzmann gas at high temperatures. All along this transition from a quantum degenerate to a classical gas, the dynamics can be captured by a kinetic equation; this contrasts with the strongly-interacting regime where the Fermi liquid and the high-temperature gas are separated by a strongly-correlated regime in which the Bogoliubov–Born–Green–Kirkwood–Yvon (BBGKY) hierarchy cannot be truncated.

Exploiting the privileged situation of the weakly-interacting gas, one can work out accurate predictions of the transport properties, that can be used, both experimentally and theoretically, as benchmarks for the strongly-correlated regime. For the transport coefficients, this requires in particular to discard the uncontrolled relaxation time approximations (RTA), and solve the kinetic equation exactly in the hydrodynamic limit.

Here we compute the shear viscosity η , thermal diffusivity κ and spin diffusivity D of a weakly-interacting Fermi gas with contact interactions in function of T/T_F , and to leading order in the s-wave scattering length a . We observe a sharp increase of the errors of the variational RTA from a few percents in the classical regime [1], to 10%–30% in the quantum regime [2, 3]. The poor accuracy of the RTA at low temperatures was noticed for Bose gases [4] but overlooked for fermions [5–8]

* hadrien.kurkjian@cnrs.fr

We obtain the exact solution of the linearized Boltzmann equation by expanding the momentum distribution $n(\mathbf{p})$ on a set of basis of orthogonal polynomials. Restricting ourselves to distributions rotationally invariant about the excitation wavevector \mathbf{q} , we use Legendre polynomials to describe the angular dependence of n ; for the radial dependence, we construct families of polynomials $\{Q_n^l(p)\}_{n \in \mathbb{N}}$ adapted to both the temperature and to the partial wave l . This very efficient decomposition of the particle distribution could be used for fast and accurate numerical solution of the kinetic equation, to study *e.g.*, time-dependent evolutions or nonlinear effects. The data and Fortran 90 source code of the numerical calculation of $\eta(T/T_F)$, $\kappa(T/T_F)$ and $D(T/T_F)$ is available at [9].

I. TRANSPORT EQUATION OF A WEAKLY-INTERACTING FERMI GAS

A. Weakly-interacting Fermi gas

We consider a gas of spin-1/2 fermions of mass m and chemical potential μ trapped in a cubic volume L^3 and interacting via contact interactions, characterized by the coupling constant g . The total equilibrium density ρ fixes the Fermi units

$$p_F = (3\pi^2 \rho)^{1/3}, \quad \epsilon_F = \frac{p_F^2}{2m} \quad (1)$$

(we use $\hbar = k_B = 1$ throughout). The Hamiltonian of the system reads:

$$\hat{H} = \hat{H}_0 + \hat{V}, \quad (2)$$

$$\hat{H}_0 = \sum_{\mathbf{p} \in \mathcal{D}, \sigma} \frac{p^2}{2m} \hat{a}_{\mathbf{p}\sigma}^\dagger \hat{a}_{\mathbf{p}\sigma} \quad (3)$$

$$\hat{V} = g \int d^3r \hat{\psi}_\uparrow^\dagger(\mathbf{r}) \hat{\psi}_\downarrow^\dagger(\mathbf{r}) \hat{\psi}_\downarrow(\mathbf{r}) \hat{\psi}_\uparrow(\mathbf{r}) = \frac{g}{L^3} \sum_{\mathbf{p}_1, \mathbf{p}_2, \mathbf{p}_3, \mathbf{p}_4 \in \mathcal{D}} \delta_{\mathbf{p}_1 + \mathbf{p}_2}^{\mathbf{p}_3 + \mathbf{p}_4} \hat{a}_{\mathbf{p}_1 \uparrow}^\dagger \hat{a}_{\mathbf{p}_2 \downarrow}^\dagger \hat{a}_{\mathbf{p}_3 \downarrow} \hat{a}_{\mathbf{p}_4 \uparrow} \quad (4)$$

where $\hat{\psi}_\sigma(\mathbf{r})$ is the field operator fermions of spin σ , and $\hat{a}_{\mathbf{p}\sigma} = \int \frac{d^3r}{\sqrt{L^3}} e^{-i\mathbf{p}\cdot\mathbf{r}} \hat{\psi}_\sigma(\mathbf{r})$ its Fourier transform. The set of momenta $\mathcal{D} = (2\pi\mathbb{Z}/L)^3$ tends to a continuum in the thermodynamic limit. To first order in perturbation theory, we relate the coupling constant g to the s-wave scattering length in the Born approximation [3, 10]

$$g = \frac{4\pi a}{m} \quad (5)$$

B. Collisional dynamics of the particle distribution

Unlike in strongly-interacting systems, the validity of the transport equation in a weakly-interacting gas is guaranteed at all temperatures and momenta by the smallness of interactions. In an homogeneous state, one may identify the phase-space distribution function to the momentum distribution of the particles

$$n_\sigma(\mathbf{p}, t) = \langle \hat{a}_{\mathbf{p}\sigma}^\dagger \hat{a}_{\mathbf{p}\sigma} \rangle \quad (6)$$

The average value $\langle \hat{O} \rangle = \text{Tr}(\hat{\rho}\hat{O})$ is taken in the state of the system $\hat{\rho}$. Within linear response theory, we assume that this state remains close to thermal equilibrium

$$\hat{\rho} = \hat{\rho}_{\text{th}}(T) + \delta\hat{\rho}, \quad \hat{\rho}_{\text{th}}(T) = \frac{e^{-\hat{H}/T}}{Z} \quad (7)$$

where Z is the partition function. The fluctuation $\delta\hat{\rho}$ is triggered by an external drive, and thus proportional to the intensity U of the driving field:

$$\hat{H}_{\text{d}} = \int d^3r U_{\sigma}(\mathbf{r}, t) \hat{\psi}_{\sigma}^{\dagger}(\mathbf{r}) \hat{\psi}_{\sigma}(\mathbf{r}) = \sum_{\mathbf{q} \in \mathcal{D}} U_{\sigma}(\mathbf{q}, t) \sum_{\mathbf{p} \in \mathcal{D}} \hat{a}_{\mathbf{p}+\mathbf{q}/2, \sigma}^{\dagger} \hat{a}_{\mathbf{p}-\mathbf{q}/2, \sigma} \quad (8)$$

where the Fourier transform of the drive is defined by $U_{\sigma}(\mathbf{q}) = \int d^3r e^{-i\mathbf{q} \cdot \mathbf{r}} U_{\sigma}(\mathbf{r})/L^3$.

In an inhomogeneous state, the phase-space distribution $\hat{n}_{\sigma}(\mathbf{p}, \mathbf{r})$ is the Wigner transform of

$$n_{\sigma}(\mathbf{p}, \mathbf{q}) = \langle \hat{a}_{\mathbf{p}-\mathbf{q}/2, \sigma}^{\dagger} \hat{a}_{\mathbf{p}+\mathbf{q}/2, \sigma} \rangle - \delta_{\mathbf{q}, 0} n_{\text{eq}} \left(\frac{p^2}{2m} + g\rho_{\sigma'}^{\text{eq}} \right) \quad (9)$$

To single-out the fluctuations, we subtract the thermal average value of the operator $\hat{a}^{\dagger}\hat{a}$ (nonzero only when $\mathbf{q} = 0$):

$$\langle \hat{a}_{\mathbf{p}\sigma}^{\dagger} \hat{a}_{\mathbf{p}\sigma} \rangle_{\hat{\rho}_{\text{th}}} = n_{\text{eq}} \left(\frac{p^2}{2m} + g\rho_{\sigma'}^{\text{eq}} \right) + O(g^2), \quad n_{\text{eq}}(\epsilon) = \frac{1}{1 + e^{(\epsilon - \mu)/T}} \quad (10)$$

where $\rho_{\uparrow}^{\text{eq}} = \rho_{\downarrow}^{\text{eq}} = \rho_{\text{eq}}/2$ are the equilibrium densities, related to μ by the equation-of-state (see Section. II A).

We explain in Ref. [11] how to obtain the time-evolution of $n_{\sigma}(\mathbf{p}, \mathbf{q})$ in the Born-Markov approximation (see also Sec. I.4. in [12]). The hierarchy of equations of motion connecting the few-body correlation functions is controlled by the coupling constant g , such that the one-body correlation functions are of order g^0 , the two-body correlations of order g^1 and so-on. To leading order in g , the hierarchy can therefore be truncate at the level of one- and two-body correlations, *i.e.* quadratic ($\hat{a}^{\dagger}\hat{a}$) and quartic ($\hat{a}^{\dagger}\hat{a}^{\dagger}\hat{a}\hat{a}$) operators [13]. In contrast with the quasiparticle transport discussed in Ref. [11], transport in the weakly-interacting regime is supported by the bare particles colliding with the bare interaction g , and experiencing simply a mean-field shift to their eigenenergy

$$\epsilon_{\sigma}(\mathbf{p}) = \frac{p^2}{2m} + g\rho_{\sigma'}^{\text{eq}} \quad (11)$$

$$\mathcal{A}(\mathbf{p}_1, \mathbf{p}_2; \mathbf{p}_3, \mathbf{p}_4) = g \quad (12)$$

The mean field shift can be absorbed by a redefinition of the chemical potential

$$\epsilon_{\sigma}(\mathbf{p}) - \mu = \frac{p^2}{2m} - \mu_0 \quad \mu = \mu_0 + g\rho_{\sigma'}^{\text{eq}} \quad (13)$$

where μ_0 is the chemical potential of the ideal Fermi gas.

The separation of scales between the Fermi energy ϵ_F and interaction energy $g\rho$ justifies a Markovian elimination of the quartic operators. We then restrict to long-wavelength physics,

retaining only the leading terms in q/k_F in the resulting equation for quadratic operators. This yields the transport equation:

$$i\frac{\partial n_\sigma}{\partial t} - \frac{\mathbf{p} \cdot \mathbf{q}}{m} n_\sigma + g \frac{\mathbf{p} \cdot \mathbf{q}}{m} \frac{\partial n_{\text{eq}}}{\partial \epsilon} \Big|_{\epsilon=\epsilon_\sigma(\mathbf{p})} (\delta\rho_{-\sigma}(\mathbf{q}) + U_\sigma(\mathbf{q})) = iI_{\text{lin},\sigma}(\mathbf{p}) \quad (14)$$

where

$$\delta\rho_{-\sigma}(\mathbf{q}) = \sum_{\mathbf{p} \in \mathcal{D}} n_{-\sigma}(\mathbf{p}, \mathbf{q}) \quad (15)$$

is the fluctuation of the spin- σ density.

The collision integral has the same structure as in the low temperature case:

$$I_{\text{lin},\sigma}(\mathbf{p}) = - \left(\Gamma(\mathbf{p}) n_\sigma(\mathbf{p}) + \frac{1}{V} \sum_{\mathbf{p}'} [E(\mathbf{p}', \mathbf{p}) n_{-\sigma}(\mathbf{p}') - S(\mathbf{p}', \mathbf{p}) (n_\sigma(\mathbf{p}') + n_{-\sigma}(\mathbf{p}'))] \right) \quad (16)$$

The quasiparticle lifetime Γ and the collision kernels E and S are given by Fermi's Golden rule:

$$\begin{aligned} \Gamma(\mathbf{p}) = 2\pi \frac{g^2}{V^2} \sum_{\mathbf{p}_2, \mathbf{p}_3, \mathbf{p}_4} \delta_{\mathbf{p} + \mathbf{p}_2, \mathbf{p}_3 + \mathbf{p}_4} \delta \left(\frac{p^2}{2m} + \frac{p_2^2}{2m} - \frac{p_3^2}{2m} - \frac{p_4^2}{2m} \right) \\ \times \left[n_{\text{eq}}(\mathbf{p}_2) (1 - n_{\text{eq}}(\mathbf{p}_3) - n_{\text{eq}}(\mathbf{p}_4)) + n_{\text{eq}}(\mathbf{p}_3) n_{\text{eq}}(\mathbf{p}_4) \right] \end{aligned} \quad (17)$$

$$\begin{aligned} E(\mathbf{p}, \mathbf{p}') = 2\pi \frac{g^2}{V} \sum_{\mathbf{p}_3, \mathbf{p}_4} \delta_{\mathbf{p} + \mathbf{p}', \mathbf{p}_3 + \mathbf{p}_4} \delta \left(\frac{p^2}{2m} + \frac{p'^2}{2m} - \frac{p_3^2}{2m} - \frac{p_4^2}{2m} \right) \\ \times \left[n_{\text{eq}}(\mathbf{p}') (1 - n_{\text{eq}}(\mathbf{p}_3) - n_{\text{eq}}(\mathbf{p}_4)) + n_{\text{eq}}(\mathbf{p}_3) n_{\text{eq}}(\mathbf{p}_4) \right] \end{aligned} \quad (18)$$

$$\begin{aligned} S(\mathbf{p}, \mathbf{p}') = 2\pi \frac{g^2}{V} \sum_{\mathbf{p}_2, \mathbf{p}_4} \delta_{\mathbf{p} + \mathbf{p}_2, \mathbf{p}' + \mathbf{p}_4} \delta \left(\frac{p^2}{2m} + \frac{p_2^2}{2m} - \frac{p'^2}{2m} - \frac{p_4^2}{2m} \right) \\ \times \left[n_{\text{eq}}(\mathbf{p}_2) (1 - n_{\text{eq}}(\mathbf{p}') - n_{\text{eq}}(\mathbf{p}_4)) + n_{\text{eq}}(\mathbf{p}') n_{\text{eq}}(\mathbf{p}_4) \right] \end{aligned} \quad (19)$$

As expected in the semi-classical regime, these expressions follow from the linearization of the Fermi-Dirac gain-loss factor $n_\uparrow(\mathbf{p})n_\downarrow(\mathbf{p}_2)(1-n_\downarrow(\mathbf{p}_3))(1-n_\uparrow(\mathbf{p}_4)) - (1-n_\uparrow(\mathbf{p}))(1-n_\downarrow(\mathbf{p}_2))n_\downarrow(\mathbf{p}_3)n_\uparrow(\mathbf{p}_4)$ for small spatial fluctuations of n_σ about n_{eq} .

We reparametrize the transport equation by extracting the density of available states $\partial n_{\text{eq}}/\partial \epsilon$:

$$n_\sigma(\mathbf{p}, \mathbf{q}) = \frac{\partial n_{\text{eq}}}{\partial \epsilon} \Big|_{\epsilon_{\text{eq}}(\mathbf{p})} \nu_\sigma(\mathbf{p}) \quad (20)$$

where the dependence of ν on \mathbf{q} is implicit. This reparametrization is unavoidable in the low temperature regime, where the particle distribution $n_\sigma(\mathbf{p})$ is peaked about p_F ; elsewhere it is rather a calculation commodity.

In the thermodynamic limit, the transport equation folds onto the integral equation

$$\left(\omega - \frac{\mathbf{p} \cdot \mathbf{q}}{m}\right) \nu_\sigma(\mathbf{p}) + g \frac{\mathbf{p} \cdot \mathbf{q}}{m} \int \frac{d^3 p'}{(2\pi)^3} \frac{\partial n_{eq}}{\partial \epsilon} \Big|_{\epsilon_{eq}(\mathbf{p}')} \nu_{-\sigma}(\mathbf{p}') + i \left\{ \Gamma(p) \nu_\sigma(\mathbf{p}) + \int \frac{d^3 p'}{(2\pi)^3} [E(\mathbf{p}, \mathbf{p}') \nu_{-\sigma}(\mathbf{p}') - S(\mathbf{p}, \mathbf{p}') [\nu_\sigma(\mathbf{p}') + \nu_{-\sigma}(\mathbf{p}')]] \right\} = -\frac{\mathbf{p} \cdot \mathbf{q}}{m} U_\sigma \quad (21)$$

where we have assumed a periodic driving $U_\sigma(\mathbf{q}, t) = U_\sigma(\mathbf{q})^{-i\omega t}$. In the general case, this equation is a 3D integral equation; here it simplifies to a 2D equation due to the azimuthal invariance.

C. Dimensionless variables and explicit expression of the collision kernel

We work in this section in temperature units, that is, with the dimensionless quantities:

$$\tilde{c} = \frac{\omega}{v_T q}, \quad \tilde{\mu}_0 = \frac{\mu_0}{T}, \quad \tilde{q} = \frac{q}{p_T}, \quad p = \frac{\|\mathbf{p}\|}{p_T}, \quad \tilde{a} = p_T a \quad (22)$$

with $v_T = \sqrt{2T/m}$ the typical thermal velocity and $p_T = mv_T$ the associated momentum. Choosing \mathbf{q} as the z -axis of our spherical frame, and exploiting the rotation invariance we parametrize the distribution ν as

$$\nu_\sigma(\mathbf{p}) = \nu_\sigma(p, \theta) \quad (23)$$

where $p = \|\mathbf{p}\|/p_T$ and $\theta = (\widehat{\mathbf{p}, \mathbf{q}})$. Note that we could replace p by an energy variable $\epsilon = p^2 - \tilde{\mu}_0$. However, since the (anti)symmetry $\epsilon \leftrightarrow -\epsilon$ about the Fermi surface disappears at nonzero temperature, there is no strong motivation to do so. Instead, keeping p as the radial variable will allow us to exploit the differentiability of the distribution ν in $p = 0$. In dimensionless units, the transport equation takes the form

$$(\tilde{c} - p \cos \theta) \nu_\sigma(p, \theta) - \frac{\tilde{a}}{\pi^2} p \cos \theta \int d^3 p' g(p') \nu_{-\sigma}(p', \theta') + \frac{i}{\omega_T \tau} \times \left(\Gamma(p) \nu_\sigma(p, \theta) + \int d^3 \tilde{p}' \left[\tilde{E}(p, p', u) \nu_{-\sigma}(p', \theta') - \tilde{S}(p, p', u) (\nu_\sigma(p', \theta') + \nu_{-\sigma}(p', \theta')) \right] \right) = -p \cos \theta U_\sigma \quad (24)$$

where $p' = \|\mathbf{p}'\|/p_T$, $g(p) = 1/4 \cosh^2((p^2 - \tilde{\mu}_0)/2)$, $u = \cos(\widehat{\mathbf{p}, \mathbf{p}'})$ and

$$\tau = \frac{\pi}{2ma^2 T^2} \quad (25)$$

is the typical collision time in the low-temperature regime. We will generalize the definition of the mean collision time to arbitrary temperature below (see Eq. (46)).

The dimensionless kernels E and S are computed in Appendix A. The result is

$$\tilde{E}(p, p', u) \equiv \left(\frac{p_T}{2\pi}\right)^3 \tau E(\mathbf{p}, \mathbf{p}') = \frac{1}{\pi p_+ \sinh \frac{\epsilon + \epsilon'}{2}} \frac{\text{ch} \frac{\epsilon}{2}}{\text{ch} \frac{\epsilon'}{2}} \ln \frac{\text{ch} \frac{\epsilon + \epsilon' + p_+ p_-}{4}}{\text{ch} \frac{\epsilon + \epsilon' - p_+ p_-}{4}} \quad (26)$$

$$\tilde{S}(p, p', u) \equiv \left(\frac{p_T}{2\pi}\right)^3 \tau S(\mathbf{p}, \mathbf{p}') = \frac{1}{2\pi p_- \sinh \frac{\epsilon - \epsilon'}{2}} \frac{\text{ch} \frac{\epsilon}{2}}{\text{ch} \frac{\epsilon'}{2}} \ln \frac{1 + e^{p_u^2 - \epsilon'}}{1 + e^{p_u^2 - \epsilon}} \quad (27)$$

with $\epsilon = p^2 - \tilde{\mu}_0$, $\epsilon' = p'^2 - \tilde{\mu}_0$, $p_{\pm} = \sqrt{p^2 \pm 2pp'u + p'^2}$, $u_- = \frac{p' - pu}{p_-}$ and $p_u = pp'\sqrt{1 - u^2}/p_-$. The expression of $\tilde{\Gamma}(p) = \tau\Gamma(\mathbf{p})$ follows from the conservation law

$$\tilde{\Gamma}(p) = - \int d^3p' (\tilde{E}(p, p', u) - 2\tilde{S}(p, p', u)) \quad (28)$$

We introduce the total density and polarisation variables

$$\nu_{\pm} = \nu_{\uparrow} \pm \nu_{\downarrow} \quad (29)$$

This diagonalizes the transport equation with respect to the spin variables:

$$(\tilde{c} - p \cos \theta) \nu_+(p, \theta) - \frac{\tilde{a}}{\pi^2} p \cos \theta \int d^3p' g(p') \nu_+(p', \theta') + \frac{i}{\omega_T \tau} \left(\tilde{\Gamma}(p) \nu_+(p, \theta) + \int d^3p' (\tilde{E}(p, p', u) - 2\tilde{S}(p, p', u)) \nu_+(p', \theta') \right) = -U_+ p \cos \theta \quad (30)$$

$$(\tilde{c} - p \cos \theta) \nu_-(p, \theta) + \frac{\tilde{a}}{\pi^2} p \cos \theta \int d^3p' g(p') \nu_-(p', \theta') + \frac{i}{\omega_T \tau} \left(\tilde{\Gamma}(p) \nu_-(p, \theta) - \int d^3p' \tilde{E}(p, p', u) \nu_-(p', \theta') \right) = -U_- p \cos \theta \quad (31)$$

where $U_{\pm} = U_{\uparrow} \pm U_{\downarrow}$.

D. Projection onto an orthogonal basis

We now project those transport equations onto an orthogonal basis of polynomials:

$$\nu_{\pm}(p, \theta) = U_{\pm} \sum_{l=0}^{+\infty} \nu_{l\pm}(p) P_l(\cos \theta) = U_{\pm} \sum_{l=0}^{+\infty} \sum_{n=l}^{+\infty} \nu_{n\pm}^l P_l(\cos \theta) Q_n^l(p) \quad (32)$$

Note ν is scaled to the intensity U of the drive, such that the coefficients $\nu_{n\pm}^l$ are dimensionless and independent of U in the linear regime $U \rightarrow 0$. The smoothness of the distribution ν in $p = 0$ implies that ν^l must be divisible by p^l . To exploit this property, we construct a different orthogonal family for each spherical harmonic l through a specific initialization condition:

$$l = 0 \quad Q_0^0 = 1, \quad Q_1^0 = p \quad (33)$$

$$l \geq 1 \quad Q_{l-1}^l = p^{l-1}, \quad Q_l^l = p^l \quad (\text{and } Q_{n < l-1}^l = 0) \quad (34)$$

The orthogonality condition is however the same for all l

$$\langle Q_n^l, Q_m^l \rangle = \delta_{nm} \|Q_n^l\|^2 \quad (35)$$

with the scalar product weighted by the (dimensionless) density of available states g :

$$\langle P, Q \rangle = \frac{1}{2} \int_{-\infty}^{\infty} p^2 dp g(p) P(p) Q(p) \quad (36)$$

The family $\{Q_n^l\}_{n \in \mathbb{N}}$ follows from the usual recurrence relation

$$Q_{n+1}^l = pQ_n^l - \xi_n^l Q_{n-1}^l \quad (37)$$

applied to the initial condition Eqs. (33)–(34). We have defined

$$\xi_n^l = \frac{\|Q_n^l\|^2}{\|Q_{n-1}^l\|^2} \quad (38)$$

We project the damping rate $\tilde{\Gamma}$, and more generally any 1D functions $\tilde{F}(p)$, according to

$$F_{nn'}^l = \frac{1}{2} \int_{-\infty}^{\infty} p^2 dp g(p) \frac{Q_n^l(p)}{\|Q_n^l\|^2} \tilde{F}(p) Q_{n'}^l(p) \quad (39)$$

For 3D tensors $\tilde{T}(\mathbf{p}, \mathbf{p}') = \tilde{T}(p, p', u = (\widehat{\mathbf{p}, \mathbf{p}'})$), such as \tilde{E} and \tilde{S} , we use

$$T_{nn'}^l = 2\pi \frac{\langle Q_n^l, T^l Q_{n'}^l \rangle}{\|Q_n^l\|^2} \quad (40)$$

with

$$T^l(p, p') = \int_{-1}^1 du P_l(u) \tilde{T}(p, p', u) \text{ and } \langle P, TQ \rangle = \frac{1}{2} \int_{-\infty}^{\infty} p^2 dp g(p) p'^2 dp' P(p) T(p, p') Q(p') \quad (41)$$

Eqs. (30)–(31) projected onto the orthogonal basis become

$$\begin{aligned} \tilde{c}\nu_{n\pm}^l - \frac{l}{2l-1} (\nu_{n-1\pm}^{l-1} + \xi_{n+1}^{l-1} \nu_{n+1\pm}^{l-1}) - \frac{l+1}{2l+3} (\nu_{n-1\pm}^{l+1} + \xi_{n+1}^{l+1} \nu_{n+1\pm}^{l+1}) &\mp \frac{4\tilde{a}\|Q_0^0\|}{\pi} \nu_{0\pm}^0 \delta_{l1} \delta_{n1} \\ &+ \frac{i}{\omega_T \tau} \sum_{n'=0}^{+\infty} \mathcal{M}_{nn'\pm}^l \nu_{n'\pm}^l = -\delta_{l1} \delta_{n1} \end{aligned} \quad (42)$$

where the collision term is now set by the matrices

$$\mathcal{M}_{nn'+}^l = \Gamma_{nn'}^l + E_{nn'}^l - 2S_{nn'}^l \quad (43)$$

$$\mathcal{M}_{nn'-}^l = \Gamma_{nn'}^l - E_{nn'}^l \quad (44)$$

Numerically, we use the conservation law Eq. (28) to rewrite $\Gamma(p)$ as an integral similar to the one giving $E_{nn'}^l$ and $S_{nn'}^l$, and rewrite the elements of \mathcal{M} in the form

$$\mathcal{M}_{nn'\pm}^l = 2\pi \int_{-1}^1 du \int p^2 dp g(p) p'^2 dp' \frac{Q_n^l(p)}{\|Q_n^l\|^2} \tilde{T}_\pm(p, p', u) [P_l(u) Q_{n'}^l(p') - P_0(u) Q_{n'}^l(p)] \quad (45)$$

with $\tilde{T}_+ = \tilde{E} - 2\tilde{S}$ and $\tilde{T}_- = -\tilde{E}$. The counter-term $P_0(u) Q_{n'}^l(p)$ coming from $\tilde{\Gamma}$ greatly improves the numerical accuracy since it compensates the the squareroot divergence of \tilde{E} and \tilde{S} in $p = p'$ and $u = \pm 1$.

E. The mean collision time across temperatures

Postponing the solution of the transport equation to Sec. II, we can already estimate the strength of the collision term ($\propto \mathcal{M}$ in Eq. (42)) relative to the rest of the transport equation. To do so, we introduce the mean collision rate $1/\tau_m$ defined as

$$\frac{1}{\tau_m} = \frac{\Gamma_{00}^0}{\tau} = \frac{\int_0^{+\infty} d\epsilon \rho(\epsilon) \Gamma(\epsilon)}{\int_0^{+\infty} d\epsilon \rho(\epsilon)} \quad (46)$$

Mathematically, this definition correspond to the projection of Γ onto the lowest orthogonal polynomial Q_0^0 (see Eq. (39) for the projection of the dimensionless rate $\tilde{\Gamma} = \tau\Gamma$), which we expect to provide the order of magnitude of the whole collision tensor \mathcal{M} . Physically, $1/\tau_m$ is defined as an energy average of Γ (expressed in function of the energy $\epsilon = p^2/2m$) weighted by the 3D density of available states $\rho(\epsilon) = -\sqrt{\epsilon} \partial n_{\text{eq}} / \partial \epsilon$. Plotted on Fig. 1 as a function of T/T_F at fixed density, the mean collision time τ_m is a monotonically decreasing function of T/T_F . At low temperature, $\Gamma_{00}^0 \xrightarrow{T \rightarrow 0} 4\pi^2/3$ such that τ_m is comparable to τ (as expected), albeit with a large numerical prefactor $3/4\pi^2 \simeq 0.08$. This explains our use of

$$\tau_\sigma = \frac{\tau}{4\pi} = \frac{\pi}{2m\sigma T^2} \quad (47)$$

with $\sigma = 4\pi a^2$ the scattering cross-section. In practice, τ_σ is numerically closer to τ_m than τ . The opposite high temperature, or classical limit, is defined by

$$T \gg T_F \quad \text{or} \quad z \equiv e^{\beta\mu} \rightarrow 0 \quad (48)$$

at fixed scattering length a . In this limit, $\Gamma_{00}^0 \underset{z \rightarrow 0}{\sim} 2\sqrt{2}z$, such that τ_m becomes proportional to the collision time of a classical binary gas of crosssections $\sigma_{\uparrow\downarrow} = \sigma = 4\pi a^2$ and $\sigma_{\uparrow\uparrow} = 0$, that is

$$\tau_m \underset{z \rightarrow 0}{\sim} \frac{\tau_{\text{HT}}}{\sqrt{2}} \quad \text{with} \quad \tau_{\text{HT}} = \frac{\tau}{2z} = \frac{1}{v_m \rho_{\uparrow}^{\text{eq}} \sigma} \quad (49)$$

We have introduced $v_m = \sqrt{8T/\pi m}$, the average velocity of the Boltzmann gas. τ_m thus interpolates from a $1/T^2$ decay at low T to a $1/\sqrt{T}$ decay at high T , as visible on Fig. 1.

II. THE HYDRODYNAMIC LIMIT

A. Equation of state of the weakly-interacting Fermi gas

As the equilibrium properties are needed to interpret the transport properties in the hydrodynamic limit, we briefly recall the equation of state of the weakly-interacting Fermi gas. In particular, we connect the Fermi-Dirac integrals with which this equation of state is usually expressed to the norm of our polynomials Q_n^l .

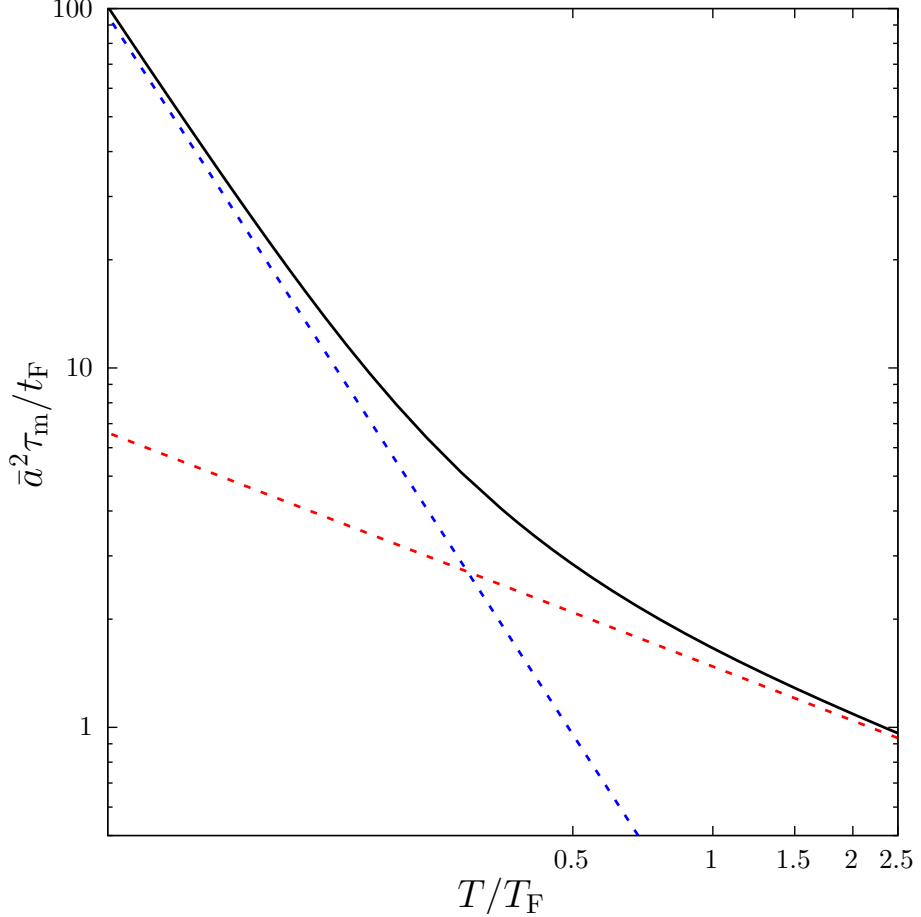


FIG. 1: The reduced mean collision time $\bar{a}^2 \tau_m / t_F$ (with $\bar{a} = k_F a$) as function of T/T_F at fixed density. It decreases monotonically first as $\tau_m \sim (3/4\pi)(T_F/T)^2 t_F / \bar{a}^2$ in the low temperature (Fermi liquid) regime (blue dashed curve), then slower, as the collision time $\tau_m \sim 1/\sqrt{2}v_m \rho_{\uparrow} \sigma$ of a hard sphere Boltzmann gas of crosssection $\sigma = 4\pi a^2$, mean velocity $v_m = \sqrt{8T/\pi m}$ and only $\uparrow\downarrow$ collisions (corresponding to $\bar{a}^2 \tau_m / t_F \sim (3\pi^2/2)\sqrt{\pi T_F/2T}$ in the Fermi units, red dashed curve).

Data for Figs. 1–2–3–4 available in [9].

The equilibrium density and pressure are related to T , the coupling constant $g = 4\pi a/m$ and $\mu_0 = \mu - g\rho_{\text{eq}}/2$ by

$$\rho_{\text{eq}} = \frac{2}{\lambda_{\text{th}}^3} \mathcal{F}_{1/2} = \frac{2}{3\pi^2} p_T^3 W_2 \quad (50)$$

$$p_{\text{eq}} = p_{\text{eq},0} + \frac{1}{4} g \rho_{\text{eq}}^2 \quad \text{with} \quad p_{\text{eq},0} = \frac{2T}{\lambda_{\text{th}}^3} \mathcal{F}_{3/2} = \frac{4}{15\pi^2} T p_T^3 W_4 \quad (51)$$

where $\lambda_{\text{th}} = \sqrt{2\pi/mT}$ is the thermal de Broglie wavelength, and $\mathcal{F}_j = \int_0^\infty t^j dt / (e^{t-\mu_0/T} + 1) / \Gamma(j+1)$ is the complete Fermi-Dirac integral. We have introduced W_n , the norm of $p^{n/2}$ in the scalar product Eq. (36), related to \mathcal{F}_j by:

$$W_n \equiv \|p^{n/2}\|^2 = \left(\frac{n+1}{2}\right) \Gamma\left(\frac{n+1}{2}\right) \frac{\mathcal{F}_{(n-1)/2}}{2} \quad (52)$$

For the internal energy u_{eq} , kinetic energy e_{eq} , and entropy s_{eq} , all per unit volume, we have

$$e_{\text{eq}} = \frac{3}{2}p_{\text{eq},0} \quad (53)$$

$$u_{\text{eq}} = e_{\text{eq}} + \frac{1}{4}g\rho_{\text{eq}}^2 \quad (54)$$

$$s_{\text{eq}} = \frac{\frac{5}{2}\mathcal{F}_{3/2} - \frac{\mu_0}{T}\mathcal{F}_{1/2}}{\mathcal{F}_{1/2}}\rho_{\text{eq}} \quad (55)$$

Since the entropy per particle $s_{\text{eq}}/\rho_{\text{eq}}$ is a function only of μ_0/T , isentropic transformations ($dS = 0$) are characterized by $d(\mu_0/T) = 0$. Differentiating Eqs. (50)–(51), we deduce the isentropic compressibility $\chi_s = \rho_{\text{eq}}(\partial\rho/\partial P)_S$:

$$\frac{1}{\rho_{\text{eq}}\chi_s} = \frac{5T}{3}\frac{\mathcal{F}_{3/2}}{\mathcal{F}_{1/2}} + \frac{g\rho_{\text{eq}}}{2} = \frac{2W_4}{3W_2} + \frac{g\rho_{\text{eq}}}{2} \quad (56)$$

From Eq. (53), we can also extract the specific heat

$$\frac{c_V}{V} \equiv \left(\frac{\partial e_{\text{eq}}}{\partial T}\right)_{\rho_{\text{eq}}} = \frac{3\rho_{\text{eq}}}{2}\left(\frac{W_4}{W_2} - \frac{W_2}{W_0}\right) = \frac{3\rho_{\text{eq}}}{2}\frac{\|Q_2^0\|^2}{\|Q_1^1\|^2} \quad (57)$$

Finally, the polarisation susceptibility is given by

$$\chi_p \equiv \left(\frac{\partial(\rho_{\uparrow}^{\text{eq}} - \rho_{\downarrow}^{\text{eq}})}{\partial(\mu_{\uparrow} - \mu_{\downarrow})}\right)_{\mu_{\downarrow}=0,T} = \frac{1}{T\lambda_T^3}\mathcal{F}_{-1/2} = \frac{p_T^3}{2T}\frac{W_0}{\pi^2}. \quad (58)$$

B. Conserved quantities and collision times

In hydrodynamic flows, the particle distribution n can be summarized by the conserved quantities, which are insensitive to collisions, and whose evolution is described by Navier-Stokes equations. There are four conserved quantities, three in the total density sector: ν_{0+}^0 , ν_{1+}^1 and ν_{2+}^0 proportional respectively to the total density, the total velocity and the total energy density, and one in the spin sector: ν_{0-}^0 , proportional to the polarisation. Mathematically, these conserved quantities are the projection of the distribution ν onto the four zero eigenfunctions of the collision kernel, namely $P_1(\cos\theta)Q_1^1(p) = p\cos\theta$, $P_0(\cos\theta)Q_2^0(p) = p^2$, and $P_0(\cos\theta)Q_0^0(p) = 1$ which is an eigenfunction in both the total density and spin sector. The restriction of the transport equation (42) to these conserved quantities gives

$$\tilde{c}\nu_{0+}^0 - \frac{\xi_1^1}{3}\nu_{1+}^1 = 0 \quad (59)$$

$$\tilde{c}\nu_{1+}^1 - (\nu_{0+}^0 + \xi_2^0\nu_{2+}^0) - \frac{2}{5}\xi_2^2\nu_{2+}^2 - \frac{4\tilde{a}\|Q_0^0\|^2}{\pi}\nu_{0+}^0 = 1 \quad (60)$$

$$\tilde{c}\nu_{2+}^0 - \frac{1}{3}(\nu_{1+}^1 + \xi_3^1\nu_{3+}^1) = 0 \quad (61)$$

in the total density sector, and

$$\tilde{c}\nu_{0-}^0 - \frac{\xi_1^1}{3}\nu_{1-}^1 = 0 \quad (62)$$

in the spin sector.

The non conserved quantities which introduce dissipation in these systems are (ν_{3+}^1, ν_{2+}^2) for the spin-symmetric conserved quantities and ν_{1-}^1 for the polarisation. We shall designate as the *first non conserved quantities*, those three components of ν , and those that are collisionally coupled to them:

$$\vec{\nu}_+^2 = (\nu_{n+}^2)_{n \geq 2} \quad (63)$$

$$\vec{\nu}_{+,\perp}^1 = (\nu_{n+}^1)_{n \geq 3} \quad (64)$$

$$\vec{\nu}_-^1 = (\nu_{n-}^1)_{n \geq 1} \quad (65)$$

In the hydrodynamic limit, the first non-conserved quantities are subleading in $O(\omega_T \tau)$ and can be approximated by

$$\vec{\nu}_+^2 = -\frac{2i}{3}(\omega_T \tau) \nu_{1+}^1 \frac{1}{\mathcal{M}_+^2} \vec{u}_2 + O(\omega_T \tau)^2 \quad (66)$$

$$\vec{\nu}_{+,\perp}^1 = -i(\omega_T \tau) \nu_{2+}^0 \frac{1}{\mathcal{M}_{+,\perp}^1} \vec{u}_3 + O(\omega_T \tau)^2 \quad (67)$$

$$\vec{\nu}_-^1 = i(\omega_T \tau) \left[1 - \nu_{0-}^0 \left(1 - \frac{4\tilde{a}}{\pi} \|Q_0\|^2 \right) \right] \frac{1}{\mathcal{M}_-^1} \vec{u}_1 + O(\omega_T \tau)^2 \quad (68)$$

where $\vec{u}_n = (\delta_{n'n})_{n' \in \mathbb{N}}$ are the units vectors of our basis. The matrices $(\mathcal{M}_{nn'}^l)_{nn'>l}$ are restricted. In Eq. (67), $\mathcal{M}_{+,\perp}^1 = (\mathcal{M}_{+,\perp}^1)_{n,n'>3}$ is the restriction of \mathcal{M}_+^1 to the subspace orthogonal to Q_1 (the zero-eigenfunction associated to the total velocity), where it is then invertible.

From (66–68), we extract the components $(\nu_{3+}^1, \nu_{2+}^2, \nu_{1,-}^1)$ needed to close the system of equations on the conserved quantities. Each of them is associated to a distinct projection of $1/\mathcal{M}$, which we write as a collision time:

$$\nu_{2,+}^2 = -\frac{2i}{3} \nu_{1+}^1 (\omega_T \tau_\eta) \quad \text{with} \quad \frac{\tau_\eta}{\tau} = \vec{u}_2 \frac{1}{\mathcal{M}_+^2} \vec{u}_2 \quad (69)$$

$$\nu_{3,+}^1 = -i \nu_{2+}^0 (\omega_T \tau_\kappa) \quad \text{with} \quad \frac{\tau_\kappa}{\tau} = \vec{u}_3 \frac{1}{\mathcal{M}_{+,\perp}^1} \vec{u}_3 \quad (70)$$

$$\nu_{1,-}^1 = i(1 - \nu_{0-}^0) (\omega_T \tau_D) \quad \text{with} \quad \frac{\tau_D}{\tau} = \vec{u}_1 \frac{1}{\mathcal{M}_-^1} \vec{u}_1 \quad (71)$$

C. Relaxation time approximation and higher truncations

Below, we shall compare the exact collision times τ_η , τ_κ , τ_D to their value τ_η^0 , τ_κ^0 , τ_D^0 in the variational RTA, also called “first approximation” by Ref. [14]. This first approximation is obtained by truncating the particle distribution to the lowest Q_n^l polynomial:

$$\nu(p, \theta) \approx \sum_{l=0}^{+\infty} \nu_l^l P_l(\cos \theta) Q_l^l(p) \quad (72)$$

This amounts to replacing the matrices \mathcal{M}_\pm^l by numbers corresponding to their first nonzero diagonal coefficients:

$$\frac{\tau_\eta^0}{\tau} = \frac{1}{\mathcal{M}_{22+}^2} \quad (73)$$

$$\frac{\tau_\kappa^0}{\tau} = \frac{1}{\mathcal{M}_{33+}^{1,\perp}} \quad (74)$$

$$\frac{\tau_D^0}{\tau} = \frac{1}{\mathcal{M}_{11-}^1} \quad (75)$$

The first approximation can be systematically improved in our formalism by including higher Q_n polynomials:

$$\nu(p, \theta) \approx \sum_{l=0}^{+\infty} \sum_{n=l}^{l+n_{\max}} \nu_n^l P_l(\cos \theta) Q_n^l(p) \quad (76)$$

The convergence of $\tau_\eta^{n_{\max}}, \tau_\kappa^{n_{\max}}, \tau_D^{n_{\max}}$ to the exact value is rather slow in the low temperature limit $\tau_\eta^{n_{\max}} - \tau_\eta = O(1/n_{\max})$ and much faster in the high temperature limit.

D. Navier-Stokes equations at intermediate temperatures

Reinjecting Eqs. (69–71) in (59–61), we get the Naviers-Stokes equations in projected, dimensionless form:

$$\tilde{c}\nu_{0+}^0 - \frac{\xi_1^1}{3}\nu_{1+}^1 = 0 \quad (77)$$

$$\tilde{c}\nu_{1+}^1 - \left(1 + \frac{4\tilde{a}}{\pi}||Q_0^0||^2\right)\nu_{0+}^0 - \xi_2^0\nu_{2+}^0 - 1 = -\frac{4i\omega_T\tau_\eta}{15}\xi_2^2\nu_{1+}^1 + O(\omega_T\tau)^2 \quad (78)$$

$$\tilde{c}\nu_{2+}^0 - \frac{1}{3}\nu_{1+}^1 = -\frac{i\omega_T\tau_\kappa}{3}\xi_3^1\nu_{2+}^0 + O(\omega_T\tau)^2 \quad (79)$$

$$\tilde{c}\nu_{0-}^0 = \frac{i}{3}\xi_1^1\omega_T\tau_D - \frac{i}{3}\xi_1^1\omega_T\tau_D \left(1 - \frac{4\tilde{a}}{\pi}||Q_0||^2\right)\nu_{0-}^0 + O(\omega_T\tau)^3 \quad (80)$$

where we have gathered the leading terms of ballistic transport on the left-hand side, and the subleading dissipative terms (in $O(\omega_T\tau)$) on the right-hand side. Since it is hard to recognize the Naviers-Stokes equations in this form, we switch back to the physical units by introducing the usual variables of the hydrodynamical system: the two densities $\rho_\sigma(\mathbf{r}, t)$, the average velocity $v_\parallel(\mathbf{r}, t)$ in the direction of \mathbf{q} and the kinetic energy density $e(\mathbf{r}, t)$. Since we have worked all along in the linear response regime, our Navier-Stokes equations are expressed in terms of the linearized fields $\delta\rho_\sigma = \rho_\sigma - \rho_{\text{eq}}/2$ and $\delta e = e - e_{\text{eq}}$. The link between the component $\nu_{n,\pm}^l$ of the particle

distribution and the hydrodynamic fields is then

$$\delta\rho_{\pm} \equiv \int \frac{d^3p}{(2\pi)^3} (n_{\mathbf{p}\uparrow} \pm n_{\mathbf{p}\downarrow}) = -\frac{\|P_0\|^2 \|Q_0^0\|^2 p_T^3 U_{\pm}}{(2\pi)^2 T} \nu_{0,\pm}^0 \quad (81)$$

$$\rho_0 v_{\parallel} \equiv \int \frac{d^3p}{(2\pi)^3} \frac{\mathbf{p} \cdot \mathbf{q}}{mq} (n_{\mathbf{p}\uparrow} + n_{\mathbf{p}\downarrow}) = -\frac{\|P_1\|^2 \|Q_1^1\|^2 p_T^2 U_{+}}{2\pi^2} \nu_{1,+}^1 \quad (82)$$

$$\delta e \equiv \int \frac{d^3p}{(2\pi)^3} \frac{p^2}{2m} (n_{\mathbf{p}\uparrow} + n_{\mathbf{p}\downarrow}) = -\frac{\|P_0\|^2 p_T^3 U_{+}}{(2\pi)^2} (\|Q_2^0\|^2 \nu_{2,+}^0 + \|Q_1^1\|^2 \nu_{0,+}^0) \quad (83)$$

where $\|P_l\|^2 = 2/(2l + 1)$. The last equation on the energy density can be reformulated by eliminating δe in favor of the fluctuation δT of the temperature:

$$\delta e = \left(\frac{\partial e_{\text{eq}}}{\partial T} \right)_{\rho_{+}} \delta T + \left(\frac{\partial e_{\text{eq}}}{\partial \rho_{+}} \right)_T \delta \rho_{+} \quad (84)$$

Using Eqs. (51)–(53) and (57) from the equation of state, we obtain

$$\delta T = -\frac{U_{+}}{2} \nu_{2,+}^0 \quad (85)$$

Converting Eqs. (78–80) to the physical variables, and performing the inverse space-time Fourier transform, we obtain:

$$\frac{\partial \rho_{+}}{\partial t} + \rho_{\text{eq}} \frac{\partial v_{\parallel}}{\partial z} = 0 \quad (86)$$

$$m \rho_{\text{eq}} \frac{\partial v_{\parallel}}{\partial t} + \frac{\partial p}{\partial z} - \sum_{\sigma} \rho_{\sigma}^{\text{eq}} \frac{\partial U_{\sigma}}{\partial z} = \frac{4}{3} \eta \frac{\partial^2 v_{\parallel}}{\partial z^2} \quad (87)$$

$$\frac{\partial u}{\partial t} + (u_{\text{eq}} + p_{\text{eq}}) \frac{\partial v_{\parallel}}{\partial z} = \kappa \frac{\partial^2 T}{\partial z^2} \quad (88)$$

$$\frac{\partial \rho_{-}}{\partial t} = D \frac{\partial^2 \rho_{-}}{\partial z^2} + D \chi_p \frac{\partial^2 U_{-}}{\partial z^2} \quad (89)$$

where $u(\mathbf{r}, t) = u_{\text{eq}} + \delta e(\mathbf{r}, t) + \frac{1}{2} g \rho_{\text{eq}} \delta \rho_{+}(\mathbf{r}, t)$ is the local internal energy per unit volum. We have use the fact the transport of the interaction energy is dissipativeless

$$\frac{\partial(u - e)}{\partial t} + (p_{\text{eq}} + u_{\text{eq}} - p_{\text{eq},0} - e_{\text{eq}}) \frac{\partial v_{\parallel}}{\partial z} = 0 \quad (90)$$

as a consequence of the continuity equation (86).

A crucial difference with the Navier-Stokes equations at low temperature (see Eqs. (29–32) in [15]) is the coupling between the temperature and velocity fluctuations, which occurs through the terms $\partial p / \partial z$ and $(u_{\text{eq}} + p_{\text{eq}}) \partial v_{\parallel} / \partial z$ in Eq. (87) and (88) respectively. These terms vanish at low temperature since

$$p_{\text{eq}} = \frac{2}{5} \rho_{\text{eq}} \epsilon_{\text{F}} + \frac{1}{4} g \rho_{\text{eq}}^2 + O(T^2) \quad \delta p = \left(\epsilon_{\text{F}} + \frac{1}{2} g \rho_{\text{eq}} \right) \delta \rho + O(T^2) \quad (91)$$

$$u_{\text{eq}} = \frac{3}{5} \rho_{\text{eq}} \epsilon_{\text{F}} + \frac{1}{4} g \rho_{\text{eq}}^2 + O(T^2) \quad \delta u = \left(\epsilon_{\text{F}} + \frac{1}{2} g \rho_{\text{eq}} \right) \delta \rho + \frac{c_V}{V} \delta T + O(T^2) \quad (92)$$

The momentum balance Eq. (87) is then decoupled from temperature fluctuations, and the energy balance Eq. (88) folds onto a purely thermal diffusive equation (see Eq. (31) in [15]). Note that the absence of terms linear in T in the Sommerfeld expansion of u_{eq} and p_{eq} , can be seen as a consequence of the particle-hole symmetry about the Fermi surface. Without this symmetry, the thermal and momentum dynamics would remain coupled in the limit $T \rightarrow 0$.

The three transport coefficients are given by

$$\eta = p_{\text{eq},0}\tau_\eta \quad \Rightarrow \quad \bar{\eta} \equiv \frac{(k_{\text{F}}a)^2}{\rho_{\text{eq}}}\eta = \frac{2\pi}{5} \frac{W_4}{W_2} \frac{T_{\text{F}}}{T} \frac{\tau_\eta}{\tau} \quad (93)$$

$$\kappa = \frac{\|Q_3^1\|^2}{\|Q_1^1\|^2} \frac{\rho_{\text{eq}}}{2} \frac{p_T^2}{m^2} \tau_\kappa \quad \Rightarrow \quad \bar{\kappa} \equiv \frac{m(k_{\text{F}}a)^2}{\rho_{\text{eq}}}\kappa = \pi \frac{W_6 W_2 - W_4^2}{W_2^2} \frac{T_{\text{F}}}{T} \frac{\tau_\kappa}{\tau} \quad (94)$$

$$D = \frac{\rho_{\text{eq}}}{2m\chi_p} \tau_D \quad \Rightarrow \quad \bar{D} \equiv \frac{m(k_{\text{F}}a)^2}{2} D = \frac{\pi}{3} \frac{W_2}{W_0} \frac{T_{\text{F}}}{T} \frac{\tau_D}{\tau} \quad (95)$$

The first column uses the equation-of-state to provide an expression in terms of physical quantities and collision times (we did not find a simple physical quantity to eliminate the factor $\|Q_3^1\|^2$ in κ). The second column gives a practical expression of the reduced coefficients $\bar{\eta}$, $\bar{\kappa}$ and \bar{D} which are plotted on Figs. 2, 3 and 4 in function of

$$\theta = \frac{T}{T_{\text{F}}} \quad (96)$$

at fixed density ρ_{eq} . The coefficients pass through a minimum in between a $1/\theta^p$ behavior at low θ ($p = 2$ for η and D , $p = 1$ for κ) and a $\sqrt{\theta}$ behavior at high θ . The minimum is reached for $\theta_{\text{min}} \simeq 0.75, 0.3$ and 1 respectively for η , κ and D . Our results for η and κ are in numerical agreement with Ref. [8] (Fig. 6 therein); the discussion there is however limited to $z < 100$, that is $\theta > 0.2$, and thus misses the drastic increase of the deviations $\tau_\eta/\tau_\eta^0 - 1$ and $\tau_\kappa/\tau_\kappa^0 - 1$ from the RTA.

E. The Fermi liquid limit

In the low-temperature limit, the gas behaves as a trivial Fermi liquid, where the Landau quasiparticles coincide with the bare fermions. The transport coefficients were given explicitly by Ref. [2] (see also Ref. [15] for the spin diffusivity). The diagonalisation of the collision kernel for an arbitrary collision probability was performed in Refs. [16–18], and can be readily applied to the case of an isotropic probability $W \propto g^2$. Note however that Refs. [16, 17] omit the contribution of the quantum force to dissipation, thus wrongly predicting the viscosity and spin diffusivity [15].

In the low-temperature regime, we obtain large deviations from the first RTA Eq. (72), up to 25% for the thermal conductivity:

$$\tau_\eta \simeq 1.079\tau_\eta^0 + O(\theta), \quad \frac{\tau_\eta^0}{\tau} \xrightarrow{T \rightarrow 0} \frac{15}{16\pi^2}, \quad \eta = 0.5153\rho_{\text{eq}}\epsilon_{\text{F}}\tau_\sigma + O(\theta^{-1}) \quad (97)$$

$$\tau_\kappa \simeq 1.253\tau_\kappa^0 + O(\theta), \quad \frac{\tau_\kappa^0}{\tau} \xrightarrow{T \rightarrow 0} \frac{15}{32\pi^2}, \quad \kappa = 0.2493c_V v_{\text{F}}^2 \tau_\sigma + O(\theta^0) \quad (98)$$

$$\tau_D \simeq 1.124\tau_D^0 + O(\theta), \quad \frac{\tau_D^0}{\tau} \xrightarrow{T \rightarrow 0} \frac{9}{16\pi^2}, \quad D = 0.2682v_{\text{F}}^2 \tau_\sigma + O(\theta^{-1}) \quad (99)$$

where $\theta = T/T_F$ is the reduced temperature and the heat capacity $c_V = mp_F T/3$ at low temperatures.

F. The Boltzmann gas limit

We now turn to in the high-temperature limit $T \gg T_F$. All three collision times become comparable to τ_{HT} defined in Eq. (49). We have

$$\tau_\eta \simeq 1.0160\tau_\eta^0 + O(z) \quad \text{with} \quad \frac{\tau_\eta^0}{\tau_{\text{HT}}} \xrightarrow{z \rightarrow 0} \frac{5}{4\sqrt{2}} \quad (100)$$

$$\tau_\kappa \simeq 1.0253\tau_\kappa^0 + O(z) \quad \text{with} \quad \frac{\tau_\kappa^0}{\tau_{\text{HT}}} \xrightarrow{z \rightarrow 0} \frac{15}{8\sqrt{2}} \quad (101)$$

$$\tau_D \simeq 1.0268\tau_D^0 + O(z) \quad \text{with} \quad \frac{\tau_D^0}{\tau_{\text{HT}}} \xrightarrow{z \rightarrow 0} \frac{3\sqrt{2}}{4} \quad (102)$$

The exact ratios τ_η/τ_η^0 and $\tau_\kappa/\tau_\kappa^0$ agree within 10^{-4} with the result of Ref. [14] in the “fourth approximation” (see Eq. (10.21, 4) therein). The rapid convergence of $\tau_\eta^{n_{\text{max}}}$ and $\tau_\kappa^{n_{\text{max}}}$ to τ_η and τ_κ (see Eq. (76)) illustrates the power of the Q_n^l basis (which fold onto a basis of generalized Laguerre polynomials at high temperature) in summarizing the energy-dependence of the phase-space distribution. As pointed by Refs. [5, 6], the ratios Eqs. (100)–(101)–(102) are only a few percent away from unity, which contrasts with the low temperature case. Keeping these exact ratio to express the transport coefficients, we obtain

$$\eta = \frac{5}{2\sqrt{2}} \frac{\tau_\eta}{\tau_\eta^0} \frac{T}{v_m \sigma}, \quad \bar{\eta} = \frac{15\pi^{3/2}}{32\sqrt{2}} \frac{\tau_\eta}{\tau_\eta^0} \theta^{1/2} \quad (103)$$

$$\kappa = \frac{75\sqrt{2}}{16} \frac{\tau_\kappa}{\tau_\kappa^0} \frac{T}{m \sigma v_m}, \quad \bar{\kappa} = \frac{225\pi^{3/2}}{128\sqrt{2}} \frac{\tau_\kappa}{\tau_\kappa^0} \theta^{1/2} \quad (104)$$

$$D = \frac{3\sqrt{\pi}}{8} \frac{\tau_D}{\tau_D^0} \sqrt{\frac{T}{m}} \frac{1}{\rho_{\text{eq}} \sigma}, \quad \bar{D} = \frac{9\pi^{3/2}}{64\sqrt{2}} \frac{\tau_D}{\tau_D^0} \theta^{1/2} \quad (105)$$

which provides the high temperature asymptotic curves (red dashed curves) in Figs. 2–3–4.

CONCLUSION

We introduced a method to exactly solve the quantum Boltzmann equation in the hydrodynamic regime, based on well chosen families of orthogonal polynomials. We applied this method to obtain exact values of the transport coefficients of a Fermi gas with contact interactions to leading order in the scattering length a , and pointed out large deviations from the relaxation time approximation in the low-temperature regime. Owing to its numerical frugality and to its natural truncation scheme, our method in a natural starting point to explore more complicated transport dynamics, such as second-order hydrodynamics [19–22], collisionless regimes, or non linear flows.

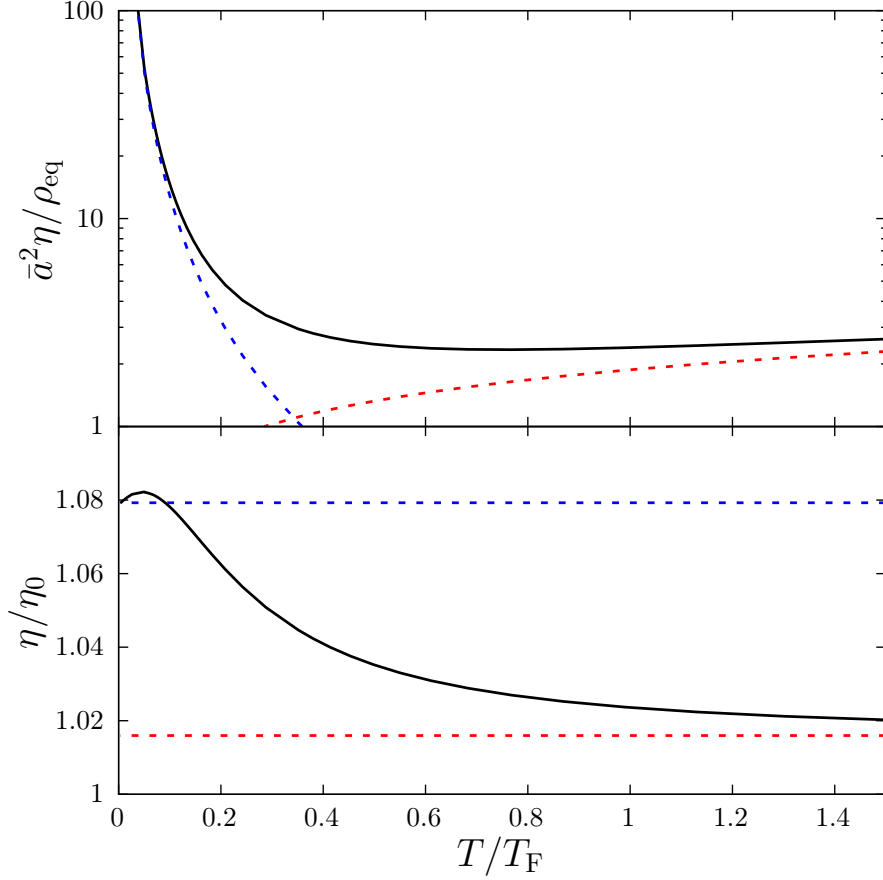


FIG. 2: (Top panel) The reduced viscosity $\bar{\eta} \equiv \bar{a}^2 \eta / \rho_{\text{eq}}$ (with $\rho_{\text{eq}} = k_F^3 / 3\pi^2$ the total density and $\bar{a} = k_F a$) as a function of $\theta = T/T_F$ at fixed density. The limiting behaviors are

$$\bar{\eta} \underset{\theta \rightarrow 0}{\sim} (2\pi/5)(\tau_\eta/\tau)/\theta^2 \approx 0.1288/\theta^2 \quad (\text{blue dashed curve})$$

$\bar{\eta} \underset{\theta \rightarrow +\infty}{\sim} (3\pi^{3/2}/8)(\tau_\eta/\tau_{\text{HT}})\sqrt{\theta} \approx 1.875\sqrt{\theta}$ (red dashed curve). (Bottom) Ratio of the exact value to the first approximation $\eta/\eta_0 = \tau_\eta/\tau_\eta^0$ (see Eq. (72)), showing the sharp deviation from unity at low temperature.

ACKNOWLEDGMENTS

H.K. acknowledges support from the French Agence Nationale de la Recherche (ANR), under grant ANR-23-ERCS-0005 (project DYFERCO)

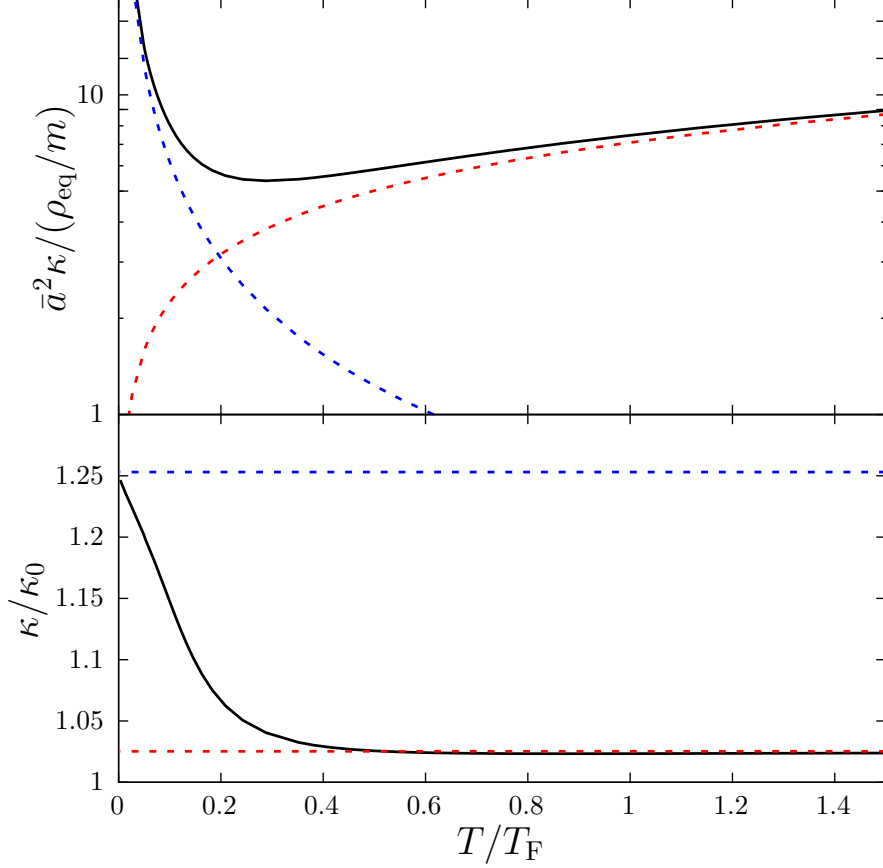


FIG. 3: (Top panel) The reduced thermal conductivity $\bar{\kappa} \equiv m \bar{a}^2 \kappa / \rho_{\text{eq}}$ as a function of $\theta = T/T_{\text{F}}$ at fixed density. The limiting behaviors are $\bar{\kappa} \underset{\theta \rightarrow 0}{\sim} (\pi^3/3)(\tau_{\kappa}/\tau)/\theta \approx 0.616/\theta$ (blue dashed curve) and $\bar{\kappa} \underset{\theta \rightarrow +\infty}{\sim} (15\pi^{3/2}/16)(\tau_{\kappa}/\tau_{\text{HT}})\sqrt{\theta} \approx 7.09\sqrt{\theta}$. (Bottom) Ratio of the exact value to the first approximation $\kappa/\kappa_0 = \tau_{\kappa}/\tau_{\kappa}^0$ (see Eq. (72)).

Appendix A: Analytic expression of the collision kernel

We detail here the derivation of Eqs. (26)–(27) on the dimensionless collision kernels \tilde{E} and \tilde{S} :

$$\tilde{E}(\tilde{p}, \tilde{p}', u) = \frac{2}{\pi^2} \int d^3 \tilde{p}_3 d^3 \tilde{p}_4 \delta(\tilde{\mathbf{p}} + \tilde{\mathbf{p}}' - \tilde{\mathbf{p}}_3 - \tilde{\mathbf{p}}_4) \delta(\tilde{p}^2 + \tilde{p}'^2 - \tilde{p}_3^2 - \tilde{p}_4^2) [n(\tilde{p}'^2) (1 - n(\tilde{p}_3^2) - n(\tilde{p}_4^2)) + n(\tilde{p}_3^2) n(\tilde{p}_4^2)] \quad (\text{A1})$$

$$\tilde{S}(\tilde{p}, \tilde{p}', u) = \frac{2}{\pi^2} \int d^3 \tilde{p}_2 d^3 \tilde{p}_4 \delta(\tilde{\mathbf{p}} + \tilde{\mathbf{p}}_2 - \tilde{\mathbf{p}}' - \tilde{\mathbf{p}}_4) \delta(\tilde{p}^2 + \tilde{p}_2^2 - \tilde{p}'^2 - \tilde{p}_4^2) [n(\tilde{p}_2^2) (1 - n(\tilde{p}'^2) - n(\tilde{p}_4^2)) + n(\tilde{p}'^2) n(\tilde{p}_4^2)] \quad (\text{A2})$$

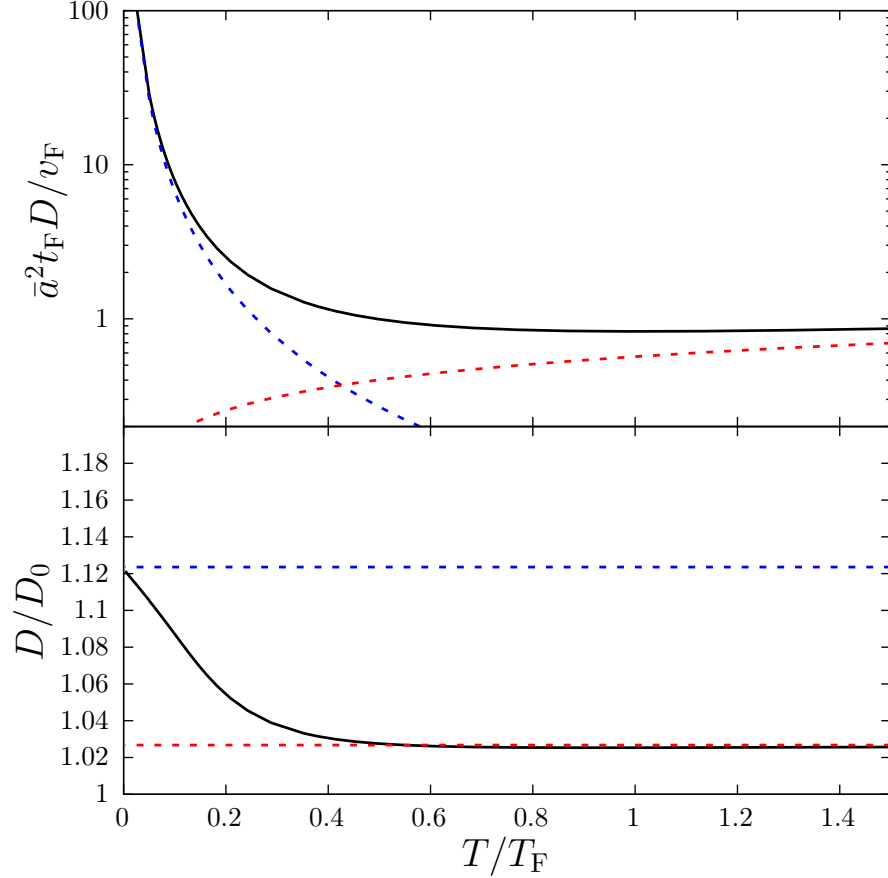


FIG. 4: (Top panel) The reduced spin diffusivity $\bar{D} \equiv m\bar{a}^2 D/2$ as a function of $\theta = T/T_F$ at fixed density. The limiting behaviors are $\bar{D} \underset{\theta \rightarrow 0}{\sim} (\pi/3)(\tau_D/\tau)/\theta^2 \approx 0.067/\theta^2$ (blue dashed curve) and $\bar{D} \underset{\theta \rightarrow +\infty}{\sim} (3\pi^{3/2}/16)(\tau_D/\tau_{\text{HT}})\sqrt{\theta} \approx 0.57\sqrt{\theta}$ (red dashed curve). (Bottom) Ratio of the exact value to the first approximation $D/D_0 = \tau_D/\tau_D^0$ (see Eq. (72)).

a. Calculation of \tilde{E} To treat the energy-momentum conservation in \tilde{E} , we introduce the variables

$$\tilde{\mathbf{p}}_3 = \frac{\mathbf{K} + \mathbf{y}}{\sqrt{2}} \quad \tilde{\mathbf{p}}_4 = \frac{\mathbf{K} - \mathbf{y}}{\sqrt{2}} \quad (\text{A3})$$

Momentum conservation fixes $\mathbf{K} = (\tilde{\mathbf{p}} + \tilde{\mathbf{p}}')/\sqrt{2}$ and energy conservation $y = \|\tilde{\mathbf{p}} - \tilde{\mathbf{p}}'\|/\sqrt{2}$. Locating \mathbf{y} in a spherical frame of axis \mathbf{K} , there remains to integrate over $u_y = \cos(\mathbf{K}, \mathbf{y})$:

$$\begin{aligned} \tilde{E}(\tilde{p}, \tilde{p}', u) = \frac{1}{\pi \tilde{p}_-} \int_0^1 du_y \left\{ n(\tilde{p}'^2) \left[1 - n \left(\frac{\tilde{p}_+^2 + \tilde{p}_-^2 + 2\tilde{p}_+\tilde{p}_-u_y}{2} \right) - n \left(\frac{\tilde{p}_+^2 + \tilde{p}_-^2 - 2\tilde{p}_+\tilde{p}_-u_y}{2} \right) \right] \right. \\ \left. + n \left(\frac{\tilde{p}_+^2 + \tilde{p}_-^2 + 2\tilde{p}_+\tilde{p}_-u_y}{2} \right) n \left(\frac{\tilde{p}_+^2 + \tilde{p}_-^2 - 2\tilde{p}_+\tilde{p}_-u_y}{2} \right) \right\} \quad (\text{A4}) \end{aligned}$$

where $\mathbf{p}_\pm = \mathbf{p} \pm \mathbf{p}'$. We have used the azimuthal invariance of the integrand, and the symmetry $u_y \leftrightarrow -u_y$. This integral can be evaluated analytically, which results in Eq. (26).

b. *Calculation of \tilde{S}* For \tilde{S} , where \mathbf{p} and \mathbf{p}' do not play symmetric roles, we keep \mathbf{p}_2 as the integration variable and eliminate \mathbf{p}_4 using momentum conservation. Locating \mathbf{p}_2 in a spherical frame of axis \mathbf{p}_- , we write the energy conservation constraint in the form:

$$p^2 + p_2^2 - p'^2 - (\mathbf{p} + \mathbf{p}_2 - \mathbf{p}')^2 = 2p_-(p_2 u_2 - p' u_-) \quad (\text{A5})$$

with $u_2 = \cos(\mathbf{p}_2, \mathbf{p}_-)$ and $u_- = \cos(\mathbf{p}', \mathbf{p}_-) = (\tilde{p}' - \tilde{p}u)/\tilde{p}_-$. Using the Dirac function to integrate over u_2 , there remains an integral over $\epsilon_2 = p_2^2$ limited to $\epsilon_2 > p'^2 u_-^2$:

$$\tilde{S}(\tilde{p}, \tilde{p}', u) = \frac{1}{\pi \tilde{p}_-} \int_{p'^2 u_-^2}^{+\infty} d\epsilon_2 \left\{ n(\epsilon_2) [1 - n(p'^2) - n(\epsilon_2 + p^2 - p'^2)] + n(p'^2) n(\epsilon_2 + p^2 - p'^2) \right\} \quad (\text{A6})$$

which finally results in Eq. (27).

Appendix B: Boltzmann gas limit of the projected transport equation

We detail here the high temperature limit of the transport equation, from which we obtained the asymptotic behaviors of the transport coefficient in Sec. II F.

The (dimensionless) collision kernel \tilde{E} and \tilde{S} , as well as the damping rate $\tilde{\Gamma}$, scale as $z = e^{\mu/T}$ in this limit:

$$\tilde{E}(\tilde{p}, \tilde{p}', u) \underset{z \rightarrow 0}{\sim} z E_{\text{HT}}(\tilde{p}, \tilde{p}', u), \quad \tilde{E}_{\text{HT}}(\tilde{p}, \tilde{p}', u) = \frac{\tilde{p}_-}{\pi} e^{-\tilde{p}'^2} \quad (\text{B1})$$

$$\tilde{S}(\tilde{p}, \tilde{p}', u) \underset{z \rightarrow 0}{\sim} z S_{\text{HT}}(\tilde{p}, \tilde{p}', u), \quad \tilde{S}_{\text{HT}}(\tilde{p}, \tilde{p}', u) = \frac{1}{\pi \tilde{p}_-} e^{-\tilde{p}'^2 u_-^2} \quad (\text{B2})$$

$$\tilde{\Gamma}(\tilde{p}) \underset{z \rightarrow 0}{\sim} z \Gamma_{\text{HT}}(\tilde{p}), \quad \tilde{\Gamma}_{\text{HT}}(\tilde{p}) = e^{-\tilde{p}^2} + \frac{(1 + 2\tilde{p}^2)\sqrt{\pi} \text{erf}(\tilde{p})}{2\tilde{p}} \quad (\text{B3})$$

where we recall that $\mathbf{p}_- = \mathbf{p} - \mathbf{p}'$ and $u_- = (p' - pu)/p_-$. We then rescale the collision time $\tau \rightarrow \tau_{\text{HT}} = \tau/2z$ (see Eq. (49)), and redefine the orthogonal polynomials using a scalar product weighted by the Maxwell-Boltzmann distribution instead of the Fermi-Dirac:

$$\langle P, Q \rangle_{\text{HT}} = \frac{1}{2} \int_{-\infty}^{\infty} p^2 dpe^{-p^2} P(p)Q(p) \quad (\text{B4})$$

The projected transport equation has the same structure as Eq. (42), except that the mean-field force $\propto g\delta\rho_\sigma$ becomes negligible in this limit:

$$\begin{aligned} \tilde{c}\nu_{n\pm}^l - \frac{l}{2l-1} (\nu_{n-1\pm}^{l-1} + \xi_{n+1}^{l-1} \nu_{n+1\pm}^{l-1}) - \frac{l+1}{2l+3} (\nu_{n-1\pm}^{l+1} + \xi_{n+1}^{l+1} \nu_{n+1\pm}^{l+1}) \\ + \frac{2i}{\omega_T \tau_{\text{HT}}} \sum_{n'=0}^{+\infty} (\mathcal{M}_{\text{HT}})_{nn'\pm}^l \nu_{n'\pm}^l = -\delta_{l1}\delta_{n1} \end{aligned} \quad (\text{B5})$$

The high-temperature version of the collision matrix \mathcal{M}_{HT} is expressed as in Eqs. (43)–(44), with $E \rightarrow E_{\text{HT}}$, $S \rightarrow S_{\text{HT}}$ and $\Gamma \rightarrow \Gamma_{\text{HT}}$. The decomposition of the function \tilde{E}_{HT} , \tilde{S}_{HT} and $\tilde{\Gamma}_{\text{HT}}$ into the

corresponding matrices occurs exactly as in Sec. I D, simply replacing the scalar product by (B4).

- [1] H. Smith and H. Højgaard Jensen. *Transport phenomena*. Clarendon Press, 1989.
- [2] Thomas Repplinger, Songtao Huang, Yunpeng Ji, Nir Navon, and Hadrien Kurkjian. Dispersion of First Sound in a Weakly Interacting Ultracold Fermi Liquid. *Annalen der Physik*, page e00181, 2025.
- [3] Songtao Huang, Yunpeng Ji, Thomas Repplinger, Gabriel G. T. Assumpção, Jianyi Chen, Grant L. Schumacher, Franklin J. Vivanco, Hadrien Kurkjian, and Nir Navon. Emergence of Sound in a Tunable Fermi Fluid. *Phys. Rev. X*, 15:011074, Mar 2025.
- [4] Erich D. Gust and L. E. Reichl. Transport coefficients from the boson Uehling-Uhlenbeck equation. *Phys. Rev. E*, 87:042109, Apr 2013.
- [5] Matt Braby, Jingyi Chao, and Thomas Schäfer. Thermal conductivity and sound attenuation in dilute atomic Fermi gases. *Phys. Rev. A*, 82:033619, September 2010.
- [6] P. Massignan, G. M. Bruun, and H. Smith. Viscous relaxation and collective oscillations in a trapped Fermi gas near the unitarity limit. *Phys. Rev. A*, 71:033607, March 2005.
- [7] G. M. Bruun and H. Smith. Viscosity and thermal relaxation for a resonantly interacting Fermi gas. *Phys. Rev. A*, 72:043605, October 2005.
- [8] Lei Wu. A fast spectral method for the Uehling-Uhlenbeck equation for quantum gas mixtures: Homogeneous relaxation and transport coefficients. *Journal of Computational Physics*, 399:108924, 2019.
- [9] H. Kurkjian. vtemp.f90. repository hkurkjian/vtemp (commit de8a647, 2025-12-08) available at <https://github.com/hkurkjian/vtemp>.
- [10] Yvan Castin. Basic Theory Tools for Degenerate Fermi Gases. In M. Inguscio, W. Ketterle, and C. Salomon, editors, *Ultra-cold Fermi Gases*. Società Italiana di Fisica, Bologna, 2007.
- [11] Pierre-Louis Taillat and Hadrien Kurkjian. A low-energy effective Hamiltonian for Landau quasiparticles. arXiv:2511.15938, 2025.
- [12] T. Repplinger. *Density wave in a Fermi gas: phonon and plasmon, from hydrodynamic to collisionless regime*. PhD thesis, Université de Toulouse, 2024.
- [13] M. Bonitz. *Quantum Kinetic Theory*. Springer, 1998.
- [14] Sydney Chapman and Thomas George Cowling. *Transport phenomena*. Cambridge University Press, 1939.
- [15] Pierre-Louis Taillat and Hadrien Kurkjian. Exact Perturbative Expansion of the Transport Coefficients of a Normal Low-Temperature Fermi Gas with Contact Interactions. *Phys. Rev. Lett.*, 135:183402, October 2025.
- [16] G. A. Brooker and J. Sykes. Transport Properties of a Fermi Liquid. *Phys. Rev. Lett.*, 21:279–282, July 1968.
- [17] H. Højgaard Jensen, H. Smith, and J.W. Wilkins. Exact transport coefficients for a Fermi liquid. *Physics Letters A*, 27(8):532–533, 1968.

- [18] E. Egilsson and C. J. Pethick. The transition from first sound to zero sound in a normal Fermi liquid. *Journal of Low Temperature Physics*, 29(1):99–118, 1977.
- [19] C. S. Wang Chang and G.E. Uhlenbeck. The kinetic theory of gases. In J. De Boer and G.E. Uhlenbeck, editors, *Studies in statistical mechanics*, volume 5. North-Holland Publishing Company, Amsterdam, 1970.
- [20] L.S. García-Colín, R.M. Velasco, and F.J. Uribe. Beyond the Navier–Stokes equations: Burnett hydrodynamics. *Physics Reports*, 465(4):149–189, 2008.
- [21] Thomas Schäfer. Second-order fluid dynamics for the unitary Fermi gas from kinetic theory. *Phys. Rev. A*, 90:043633, October 2014.
- [22] Blaise Goutéraux and Ashish Shukla. Beyond Drude transport in hydrodynamic metals. *Phys. Rev. B*, 109:165153, April 2024.